^1H, ^2D AND ALKALI NMR STUDIES OF ALKALI NAPHTHALENE ION PAIRS

E. DE BOER and B. M. P. HENDRIKS*

Department of Physical Chemistry, University of Nijmegen, Nijmegen, The Netherlands

ABSTRACT

^1H, ^2D and alkali resonances have been performed on alkali naphthalene ion pairs in ethereal solution. Special attention is devoted to the electron spin relaxation time τ_e. It proved to be proportional to the inverse of the ion pair concentration, but not to the viscosity divided by the absolute temperature, as is predicted by the Pake–Tuttle relationship. An explanation for this behaviour is given in terms of polymolecular collision processes. The alkali resonances provided information on the sign of the alkali hyperfine splitting constants and on the contribution of the various relaxation mechanisms to the line widths. A line width analysis demonstrated that the ion pairs can be considered as static ion pairs, except for sodium naphthalene, where ion pair equilibria play an essential role.

1. INTRODUCTION

Alkali radical ion pairs have been studied in the past mainly by electron spin resonance (e.s.r.) techniques[1]. From this useful information has been obtained about the electronic structure of the ion pairs and about ion pair equilibria. During the last few years nuclear magnetic resonance (n.m.r.) experiments also have been performed on alkali radical solutions[2]. This technique offers some advantages over the e.s.r. method; the most outstanding features are the possibility of measuring the sign of the hyperfine coupling constants (h.f.s.c.s) and the more easily interpretative spectra. A drawback of the method is the necessity of large concentrations, which can, however, to some extent be circumvented by use of spin relaxers[3].

A few detailed n.m.r. studies have been carried out on alkali radical ion pairs. The system alkali biphenyl has been investigated extensively by Canters and co-workers[3,4] and the system alkali naphthalene by Takeshita and Hirota[5] and by Hendriks and co-workers[6].

In this paper we present further experimental results on the alkali naphthalene system, which shed new light on the behaviour of these concentrated solutions and made possible a more detailed analysis of the spectra. In Section 3 the relevant equations needed for the interpretation of the spectra are given. In Section 4 the experimental results are discussed.

* This paper is based on the *PhD thesis* presented by Dr B. M. P. Hendriks at the University of Nijmegen.

It is shown that at high concentrations polymolecular collision processes play an essential role in the electron spin relaxation, so that the Pake–Tuttle relation[7] is no longer valid. Fortunately the proton and deuterium line widths and the electron spin correlation times remain proportional to the inverse concentration of the radicals.

The usefulness of spin relaxers is pointed out in Section 4.2. A semi-quantitative analysis is given for the alkali line widths in Section 4.3. The analysis is based on a so-called static picture of the ion pair, except for sodium naphthalene, for which evidence is found that a dynamic model applies.

2. EXPERIMENTAL

The n.m.r. experiments were performed on a Varian DP-60-EL spectrometer. For instrumental and experimental details and for details concerning the analysis of the spectra, see refs 4 and 6. All reported line widths are corrected for modulation effects and for intermolecular broadening.

The viscosity of the sodium naphthalene (NaNl) solution in 1,2-dimethoxyethane (DME) at 25°C has been measured with Ubbelohde viscometers according to the method outlined in ref. 8 and by utilizing a glove-box (VAC HE-43-6 with drytrain VAC HE-193-1). The results are presented in *Table 1*. The viscosities are well described by the relation of Vand[9]. If not stated otherwise, all uncertainty ranges indicate a 99 per cent confidence interval.

Table 1. Viscosity of NaNl in DME at 25°C in centipoise (cP). Accuracy is 2 per cent

c(M)	0.00	0.25	0.49	0.98	1.42	1.96
η(cP)	0.443	0.528	0.697	1.17	2.13	4.93

3. THEORETICAL ASPECTS

NMR spectra of paramagnetic particles in solution are modified in two ways with respect to the spectra of the corresponding diamagnetic species. First, the resonance lines are broadened by paramagnetic relaxation mechanisms; second, the lines are shifted by the Fermi contact interaction[10].

3.1 Contact shift

For ion pairs in the doublet ground state the Fermi contact shift δ_c^0, expressed in gauss, is given by[11]

$$\delta_c^0 = -\frac{\gamma_e}{\gamma_N} a \frac{g\mu_B B_p}{4kT} \tag{1}$$

where g is the isotropic g value of the radical, a is the hyperfine splitting constant, B_p is the field at which resonance occurs and the other symbols have their usual meanings.

Since

$$a = \frac{8\pi}{3} \gamma_N \rho_N \hbar \tag{2}$$

where ρ_N is the spin density at nucleus N, the contact shift δ_c^0 is independent of the magnetic moment of the nucleus. From the direction of the shift the sign of the spin density can be inferred; a high field shift indicates a negative ρ_N; a low field shift indicates a positive ρ_N.

3.2 Line width equations for rigid ion pairs

The line widths of the absorption peaks in the n.m.r. spectrum of an ion pair are completely determined by intramolecular interactions. In general, the line width parameter T_2 can be written as a sum of three terms

$$T_2^{-1} = T_{2,\mathrm{Fc}}^{-1} + T_{2,\mathrm{Dip}}^{-1} + T_{2,\mathrm{Q}}^{-1} \tag{3}$$

the three terms representing the contributions due to the Fermi contact interaction, the anisotropic electron–nucleus dipolar interaction, and the quadrupolar interaction, respectively. For a rigid radical ion pair undergoing a rapid isotropic Brownian motion in solution, the following expressions hold for the three relaxation times[12]:

$$T_{2,\mathrm{Fc}}^{-1} = \frac{1}{4}\left(\frac{A}{\hbar}\right)^2 \left\{\tau_e + \frac{\tau_e}{1 + \omega_e^2\tau_e^2}\right\} \tag{4a}$$

$$T_{2,\mathrm{Dip}}^{-1} = \frac{1}{20}\left(\frac{B}{\hbar}\right)^2 \left\{7\tau_d + \frac{13\tau_d}{1 + \omega_e^2\tau_d^2}\right\} \tag{4b}$$

$$T_{2,\mathrm{Q}}^{-1} = \frac{3}{10}\left(\frac{C}{\hbar}\right)^2 \tau_r \tag{4c}$$

where τ_e is the electron spin correlation time and τ_d is the dipolar correlation time, defined by

$$\tau_d^{-1} = \tau_e^{-1} + \tau_r^{-1} \tag{5}$$

in which τ_r is the rotational correlation time. A, B and C are defined by

$$A = \gamma_e \hbar a$$

$$B = \left[\tfrac{1}{6}\sum_{i,j}(T_{ij})^2\right]^{\frac{1}{2}} \tag{7}$$

$$C = \left[f(I)(eQ)^2\{\tfrac{1}{6}\sum_{i,j}(V_{ij})^2\}\right]^{\frac{1}{2}} \tag{8}$$

where T_{ij} are the components of the anisotropic dipolar tensor and V_{ij} the components of the electric field gradient tensor. The factor $f(I)$ is given by $(2I + 3)/I^2(2I - 1)$ and eQ is the nuclear quadrupole moment. The other symbols have their usual meanings.

The correlation times for the alkali radical ion pair are within the range 10^{-10} to 10^{-11}s, whereas the e.s.r. frequency ω_e is about 3×10^{11} rad/s. Consequently the line widths will be proportional to a particular correlation time. The correlation times depend on the radical concentration c, the absolute temperature T and the viscosity η. According to the Debye–Einstein[13] model the dependence of τ_r on η and T is given by

$$\tau_r \sim \eta/T \tag{9}$$

while according to the model of Pake and Tuttle[7] the dependence of τ_e on c, T and η is given by

$$\tau_e \sim \frac{\eta}{T} \cdot \frac{1}{c} \tag{10}$$

From these relations it follows that the total line width will be proportional to η/T.

3.3 Line width equations for dynamic ion pairs

Configurational changes of the ion pair will modulate the intramolecular interactions described above and will therefore have an influence on the line width of the absorption peaks. Line width equations have been developed for a situation in which the alkali ion switches between only two positions, say 1 and 2. Assuming again isotropic Brownian motion, the equations read[4–6]

$$T_{2,\mathrm{Fc}}^{-1} = \tfrac{1}{4}\left[\left(\frac{\bar{A}}{\hbar}\right)^2\left\{\tau_e + \frac{\tau_e}{1+\omega_e^2\tau_c^2}\right\} + p_1p_2\left(\frac{\Delta A}{\hbar}\right)^2\left\{\tau_e' + \frac{\tau_e'}{1+(\omega_e\tau_e')^2}\right\}\right] \tag{11a}$$

$$T_{2,\mathrm{Dip}}^{-1} = \tfrac{1}{20}\left[\frac{\bar{\mathbf{T}}:\bar{\mathbf{T}}}{6\hbar^2}\left\{7\tau_d + \frac{13\tau_d}{1+\omega_e^2\tau_d^2}\right\} + p_1p_2\frac{\Delta\mathbf{T}:\Delta\mathbf{T}}{6\hbar^2}\left\{7\tau_d' + \frac{13\tau_d'}{1+(\omega_e\tau_d')^2}\right\}\right] \tag{11b}$$

$$T_{2,\mathrm{Q}}^{-1} = \tfrac{3}{10}f(I)(eQ)^2\left[\frac{\bar{\mathbf{V}}:\bar{\mathbf{V}}}{6\hbar^2}\tau_r + p_1p_2\frac{\Delta\mathbf{V}:\Delta\mathbf{V}}{6\hbar^2}\tau_r'\right] \tag{11c}$$

where

$$\left.\begin{aligned}\bar{X} &\equiv p_1X_1 + p_2X_2\\ \Delta X &= X_1 - X_2\end{aligned}\right\} X = A, \mathbf{T} \text{ or } \mathbf{V}$$

The interaction parameters for the two sites are indicated by the subscripts 1 and 2, τ_e is given by

$$\frac{1}{\tau_e'} = \frac{1}{\tau_e} + \frac{1}{\tau_1} + \frac{1}{\tau_2} = \frac{1}{\tau_e} + \frac{1}{\tau} \tag{12}$$

and similar equations hold for τ_d' and τ_r'. τ_1 and τ_2 are the residence times of the ion pair in sites 1 and 2, respectively, and are related to the occupation probabilities p_1 and p_2 by the relation $p_i = \tau_i/(\tau_1 + \tau_2)$. The notation $\mathbf{X}:\mathbf{X}$ stands for the trace of the matrix product of $\mathbf{X}$ and $\mathbf{X}$ ($\mathbf{X}:\mathbf{X} = \sum_{ij}(X_{ij})^2$).

For practical purposes it is useful to distinguish two limiting cases:

(a) $\tau \ll \tau_e, \tau_r, \tau_d$. In this case the equations reduce to

$$T_{2,\mathrm{Fc}}^{-1} = \tfrac{1}{4}\left(\frac{\bar{A}}{\hbar}\right)^2\left\{\tau_e + \frac{\tau_e}{1+\omega_e^2\tau_e^2}\right\} \tag{13a}$$

$$T_{2,\mathrm{Dip}}^{-1} = \tfrac{1}{20}\left(\frac{\overline{B}}{\hbar}\right)^2 \left\{7\tau_d + \frac{13\tau_d}{1+\omega_e^2\tau_d^2}\right\} \tag{13b}$$

$$T_{2,\mathrm{Q}}^{-1} = \tfrac{3}{10}\left(\frac{\overline{C}}{\hbar}\right)^2 \tau_r \tag{13c}$$

where $\overline{B}$ and $\overline{C}$ are defined by replacing **T** in equation (7) and **V** in equation (8) by $\overline{\mathbf{T}}$ and $\overline{\mathbf{V}}$, respectively.

These equations are formally identical with equations (4) holding for the rigid ion pair, the only difference being that now the average values of the interaction parameters occur.

Since the relevant correlation times are of the order of 10^{-10} to 10^{-11} s, the configurational life times τ_1 and τ_2 are so short that the motion of the alkali ion cannot be distinguished from a vibration of the alkali ion in the potential energy well of the ion pair. In the literature this case has been called the static case, although of course the alkali ion is still vibrating around an equilibrium position.

(b) $\tau \gg \tau_e, \tau_r$. In this case the equations reduce to

$$T_{2,\mathrm{Fc}}^{-1} = \tfrac{1}{4}\left(\frac{\overline{A^2}}{\hbar^2}\right)\left\{\tau_e + \frac{\tau_e}{1+\omega_e^2\tau_e^2}\right\} \tag{14a}$$

$$T_{2,\mathrm{Dip}}^{-1} = \tfrac{1}{20}\left[\frac{\overline{\mathbf{T}:\mathbf{T}}}{6\hbar^2}\left\{7\tau_d + \frac{13\tau_d}{1+\omega_e^2\tau_d^2}\right\}\right] \tag{14b}$$

$$T_{2,\mathrm{Q}}^{-1} = \tfrac{3}{10} f(I)\,(eQ)^2 \left[\frac{\overline{\mathbf{V}:\mathbf{V}}}{6\hbar^2}\,\tau_r\right] \tag{14c}$$

with

$$\overline{\mathbf{X}:\mathbf{X}} = p_1(\mathbf{X}_1:\mathbf{X}_1) + p_2(\mathbf{X}_2:\mathbf{X}_2)$$

and

$$\overline{A^2} = p_1 A_1^2 + p_2 A_2^2$$

The configurational life times are now so long that two different ion pairs can be discerned, often called contact, or tight, and solvent-separated, or loose, ion pairs. The equations mean that the line widths are the weighted sums of the line widths of these two ion pair species. Usually this limiting case is called the dynamic case.

4. ALKALI NAPHTHALENE ION PAIRS

Thorough n.m.r. investigations of the alkali naphthalene ion pairs were reported by Hendriks and co-workers[6]. Both proton and alkali resonances were studied with DME as solvent, although the NaNl system was also studied in tetrahydrofuran (THF). Besides proton resonance, deuterium resonance studies were carried out on completely deuterated samples. In the following sections we will focus our attention mainly on the effect extremely high concentrations have on the spin exchange process, and we will give a thorough line width analysis of the alkali resonances.

4.1 ^{1}H and ^{2}D resonance

In order to obtain an impression of the type of spectra measured we have reproduced in *Figure 1* the n.m.r. spectra resulting from ^{1}H and ^{2}D n.m.r. performed on a sample containing both normal naphthalene and perdeutero-naphthalene. The peaks have been shifted to high field pointing to a negative

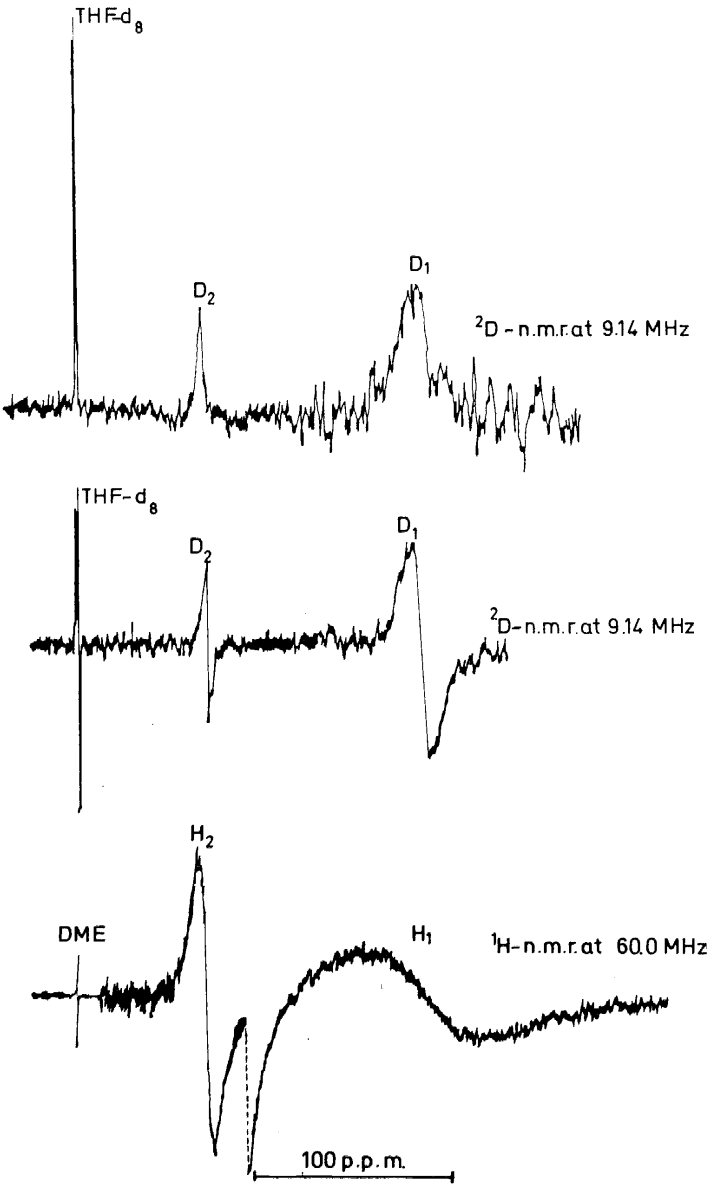

Figure 1. High-resolution and wide-line deuterium and wide-line proton spectra of a solution containing 1.63 M naphthalene and 0.62 M perdeutero-naphthalene in DME, which was completely reduced with Na. THF-d8 was used as reference signal

Table 2. ^{1}H and ^{2}D line widths (in rad/s) for the NaNl–DME mixed sample (2.25 M)

	H_1, D_1	H_2, D_2
T_{2H}^{-1}	33..000 ± 1800	4800 ± 300
T_{2D}^{-1}	850 ± 60	160 ± 10
$T_{2D,Q}^{-1}$	—	50 ± 15

spin density at the proton nuclei. The absolute values of the h.f.s.c.s are in agreement with e.s.r. data[6]. Also, it is clear that the shifts are independent of the magnetic moment of the nucleus and that the resolution in the ^{2}D spectra is much better than in the ^{1}H spectra. In *Table 2* we have listed the experimental T_2 values. From the ^{1}H and the ^{2}D line width the quadrupolar contribution to the ^{2}D line width ($T_{2D,Q}^{-1}$) has been calculated, by use of the formula

$$T_{2D,Q}^{-1} = T_{2D}^{-1} - \left(\frac{\gamma_D}{\gamma_H}\right)^2 T_{2H}^{-1} \tag{15}$$

Using equation (4c) and setting the quadrupole coupling constant (q.c.c.) of the deuteron equal to 0.19 MHz[6a] and the asymmetry parameter $(V_{xx} - V_{yy})/V_{zz}$ equal to zero, one derives that $\tau_r = (90 \pm 30) \times 10^{-12}$ s at 30°C.

The line widths proved to be proportional to the square of the h.f.s.c., which points to the predominance of the Fermi contact relaxation mechanism. In accordance with this, the line widths were also proportional to the inverse of the concentration of radical ion pairs. By use of equation (4a) τ_e can be calculated, and in *Figure 2* τ_e has been plotted against $1/c$ for solutions of NaNl-h8 and of NaNl-d8 in DME. It appears that τ_e is proportional to

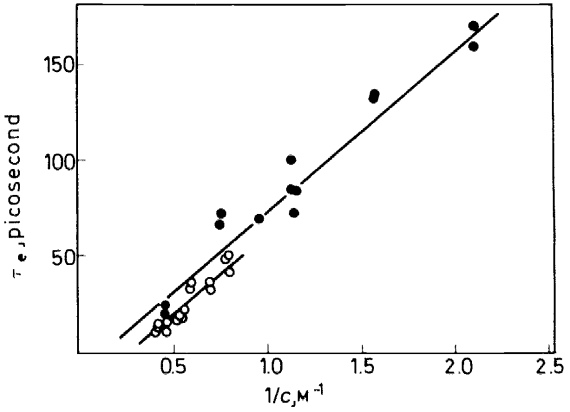

Figure 2. The electron spin correlation times measured at 30°C in solutions of NaNl-h8(○) and of NaNl-d8 (●) in DME versus the reciprocal of the radical concentration

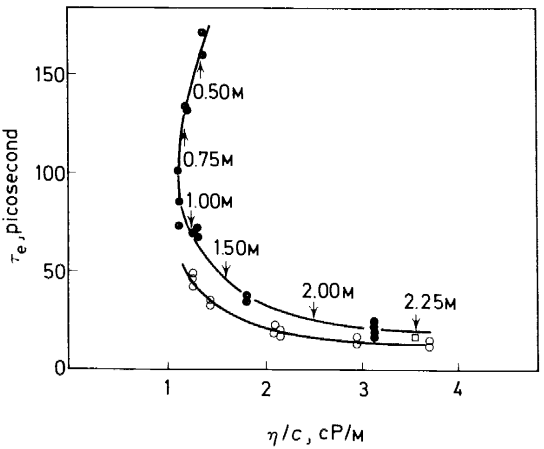

Figure 3. The electron spin correlation times at 30°C in solutions of NaNl-h8 (○) and of NaNl-d8 (●) in DME versus η/c, τ_e obtained for the 2.25 M mixed sample (□) has been presented also

$1/c$ and that the relaxation is more efficient in the proton sample. In *Figure 3* τ_e has been plotted against η/c. According to the model of Pake and Tuttle[7], a linear relationship should exist between these quantities, which is clearly not the case. At high concentrations τ_e is much smaller than expected. In their derivation of equation (10) Pake and Tuttle only considered bimolecular collision processes and furthermore assumed a constant concentration of solvent molecules. Our experiments indicate that at high concentrations polymolecular collisions are important, which shorten τ_e much faster than $1/c$ and even dominate the exponential increase of the viscosity with increasing radical concentration. Fortuitously, the over-all effect is an almost linear relationship between τ_e and $1/c$. In view of these results, it is not surprising that plots of τ_e or T_2^{-1} versus $1/c$ do not go through the origin[5,6].

At low concentrations the viscosity is almost constant and the effect of polymolecular collisions negligible. If the Pake–Tuttle model applies for these dilute solutions, we calculate for the rate constant k_e of the spin exchange process in the NaNl-d8–DME sample at 30°C a value of 13×10^9 l/mol.s. This rate constant has been calculated from

$$\tau_e^{-1} = k_e[\mathrm{Nl}^-] \tag{16}$$

and the plot shown in *Figure 2*. This value is in good agreement with the e.s.r. result of Danner[14]: $k_e = 14 \times 10^9$ l/mol.s. for KNl–DME.

4.2 Electron spin relaxation

In order for high resolution to be attained in the n.m.r. spectra of the radical ion pairs, τ_e must be small. This is accomplished by the spin–spin interaction, which increases with increasing radical concentration. Sometimes the high concentration needed for obtaining small τ_es cannot be realized. A way out of this dilemma is to measure a sparingly soluble radical in the

Table 3. ^{1}H and ^{2}D line widths (in rad/s) of the 1.2 M Bp^-/0.5 M Nl-d8$^-$ solution in DME compared with the line widths of some single-component samples

Sample	Biphenyl		Naphthalene	
	$T_{2H_2}^{-1}$	$T_{2H_3}^{-1}$	$T_{2D_1}^{-1}$	$T_{2D_2}^{-1}$
1.2 M NaBp-DME + 0.5 M NaNl-d8–DME	9800	420	1200	200
1.2 M NaBp–DME	17200	700		
1.5 M NaBp–DME	9900	360		
0.5 M NaNl-d8–DME			7200	1400
1.7 M NaNl-d8–DME			1700	280

presence of a highly soluble radical, which then may act as a spin relaxer[3]. As an example, we will discuss our results obtained on a sample containing 0.5 M Nl-d8$^-$ and 1.2 M biphenyl$^-$ (Bp^-) in DME with Na^+ as counter ion. The line widths measured at 30°C are presented in *Table 3*.

The small line width of the resonances of the Nl-d8/Bp sample with respect to the line widths measured for samples containing only one of the hydrocarbons at equal concentration demonstrates the mutually relaxing effects of the biphenylide and naphthalenide radicals. The deuteron line widths of the Nl-d8/Bp sample are smaller than the line widths of a 1.7 M Nl-d8$^-$ sample; hence, the $Bp^- \leftrightarrow Nl^-$ interaction causes a more efficient electron spin relaxation than the $Nl^- \leftrightarrow Nl^-$ interaction. However, the proton line widths of a 1.5 M Bp^- solution are already equal to the ^{1}H line widths of the biphenyl protons in the Nl-d8/Bp sample, which is 1.7 M in total radical concentration. Therefore the $Bp^- \leftrightarrow Nl^-$ interaction relaxes the electron spin less efficiently than the $Bp^- \leftrightarrow Bp^-$ interaction.

For a system of n different kinds of spin $\frac{1}{2}$ radicals (R_i) we can describe the spin exchange process by:

$$R_i(\alpha) + R_j(\beta) \underset{k_{ij}}{\overset{k_{ij}}{\rightleftarrows}} R_i(\beta) + R_j(\alpha) \tag{17}$$

where k_{ij} is the rate constant of spin exchange between the radicals R_i and R_j. From simple reaction kinetic arguments[4,5] one can derive[6] for the electron spin correlation time of radical i

$$\tau_{e_i}^{-1} = \sum_{j=1}^{n} k_{ij}[R_j] \tag{18}$$

With this notation the experimental data for our two radical system can be explained by

$$k_{Bp^-,Bp^-} > k_{Bp^-,Nl^-} > k_{Nl^-,Nl^-}$$

From our results we may conclude that both Nl^- and Bp^- can be used as a spin relaxer. The Bp^- anion is more efficient, but the solubility of this anion and the reduction potential of neutral Bp will limit its applicability to THF and stronger solvating ethers. The use of the Nl^- anion in MTHF and even weaker solvating ethers seems promising.

4.2 Alkali resonance

Alkali resonance has been carried out on $^{6}Li^{+}$, $^{7}Li^{+}$, $^{23}Na^{+}$, $^{39}K^{+}$, $^{85}Rb^{+}$, $^{87}Rb^{+}$ and $^{133}Cs^{+}$. In ref. 6 graphs have been given of the alkali h.f.s.c. versus the temperature and of the alkali line width as a function of the viscosity of the solvent divided by the absolute temperature (η_0/T)*. In general, the h.f.s.c.s increase with the temperature and the line widths increase with η_0/T, except for the cations of ^{6}Li, ^{7}Li and ^{23}Na. In *Table 4*

Table4. Survey of h.f.s.c.s, line widths and correlation times of 1.0 M NI ion pair solutions in DME. The accuracy of the h.f.s.c.s is 3 per cent and of the line widths 10 per cent unless stated otherwise

Sample	T (°C)	Isotope	a_M (G)	T_{2M}^{-1} (rad/s)	τ_e (ps)	τ_r (ps)
LiNI	30	^{6}Li	0.0033	10	85 ± 15	10–50
		^{7}Li	0.010	29		
	40	^{6}Li	0.006	13	75 ± 15	10–45
		^{7}Li	0.017	37		
	50	^{6}Li	0.010	19	65 ± 15	10–40
		^{7}Li	0.031	62		
NaNI	30	^{23}Na	0.20	1200 ± 100	70 ± 10	10–50
	60	^{23}Na	0.42	2600 ± 200	50 ± 10	10–35
KNI	30	^{39}K	0.016	800 ± 60	62 ± 6	10–50
RbNI	30	^{85}Rb	−0.175	7800 ± 200	47 ± 7	10–50
		^{87}Rb	−0.527	8700 ± 400		
CsNI	30	^{133}Cs	−1.43	10500 ± 500	52 ± 4	10–50

we have given a survey of the observed h.f.s.c.s, line widths and correlation times, all for solutions containing 1.0 M naphthalenide. The electron correlation times τ_e have been derived from the proton spectra of the anion. The lower limit of τ_r has been deduced from $T_{2D,Q}^{-1}$, the upper limit from the Debye–Einstein relation, $\tau_r = 4\pi r^3\eta/3kT$, where r is the molecular radius. We will use the data in *Table 4* for an evaluation of the systems studied. Unless indicated otherwise, we will utilize equation (13), valid for the so-called static case of a dynamic ion pair, for the analysis of the line widths. A general remark here concerns the sign of the h.f.s.c. It is positive for Li and Na, negative for Rb and Cs and, depending on the temperature, positive or negative for K. From the observed alkali h.f.s.c. the spin densities in the ns-AO of the alkali cations can be calculated by dividing the observed h.f.s.c. by the known h.f.s.c. of the alkali atoms[15]. The results are listed in *Table 5*. The spin density decreases continuously going from Na to Cs; only Li is an exception, owing to the strong solvation of this small cation. Recently the observed trend has been explained theoretically by Canters, Corvaja and de Boer[15], who pointed out that the zero-order contribution

* The concentrations of 1.0 M for the NaNI ion pair in THF and CsNI ion pair in DME mentioned in ref. 6a are erroneous. The correct values are 0.45 M for NaNI in THF and 0.5 M for CsNI in DME.

Table 5. The variation of the spin density in the metal ns-orbital with the counter ion for the alkali Nl ion pairs in DME. In the second column the values of ρ_N are given corresponding to the limits of the investigated temperature range

Metal	ρ_N	ρ_N at 30°C
Li	$(0.0–0.7) \times 10^{-3}$	0.05×10^{-3}
Na	$(0.0–2.4) \times 10^{-3}$	0.6×10^{-3}
K	$(-0.1–0.5) \times 10^{-3}$	0.2×10^{-3}
Rb	$\{-0.5–(-0.3)\} \times 10^{-3}$	-0.4×10^{-3}
Cs	$\{-1.8–(-1.5)\} \times 10^{-3}$	$\{-1.8–(-1.6)\} \times 10^{-3}$*

* Dependent on the radical concentration.

to the spin density, ρ_0, at the metal decreases more rapidly with increasing distance between the ions than the first-order contribution, ρ_1. Because ρ_0 is always positive and ρ_1 is usually negative, the spin density will become more negative with increasing distance, which explains the observed trend in the metal spin density going from Li to Cs. The usually positive temperature gradient of the alkali metal h.f.s.c. can be explained by the decreasing distance between the ions due to the decreasing solvation of the cation at elevated temperature.

Before we discuss the individual systems the trend in τ_e should be noted. It decreases gradually going from the solvent-separated LiNl ion pair to the contact ion pair CsNl. Since the distance of closest approach between the anions of two radical ion pairs is smaller for contact ion pairs than for solvated ion pairs, the exchange interaction of the unpaired electrons in the contact ion pairs is larger than in the solvent-separated ion pairs[14].

LiNl. The coincidence of the plots of $T_2^{-1}(^7\text{Li})$ and of

$$\left(\frac{\gamma_{^7\text{Li}}}{\gamma_{^6\text{Li}}}\right)^2 \times T_2^{-1}(^6\text{Li})$$

versus η_0/T (see ref. 6, Figure 8) proves that the contribution of the quadrupole interaction to the relaxation of the Li nuclei will be negligible. The Fermi contact relaxation can be calculated by use of the h.f.s.c.s and the τ_es listed in *Table 4* and equation (13a). The data are summarized in *Table 6*. It turned out that the Fermi contact relaxation is negligible. From the dipolar relaxation the distance between the Li nucleus and the aromatic plane has been calculated by comparing the experimentally determined

Table 6. Line width analysis for ^{7}LiNl in DME (1.0 M)

T (°C)	T_2^{-1} (rad/s)	$T_{2,\text{Fc}}^{-1}$ (rad/s)	$T_{2,\text{Dip}}^{-1}$ (rad/s)	τ_d (ps)	Distance (Å)
30	29	0.7	28	10–85*	2.5–4.5
40	37	1.7	35	10–75*	2.3–4.1
50	62	4.9	57	10–65*	1.9–3.4

* The upper limit corresponds with $\tau_d = \tau_e$.

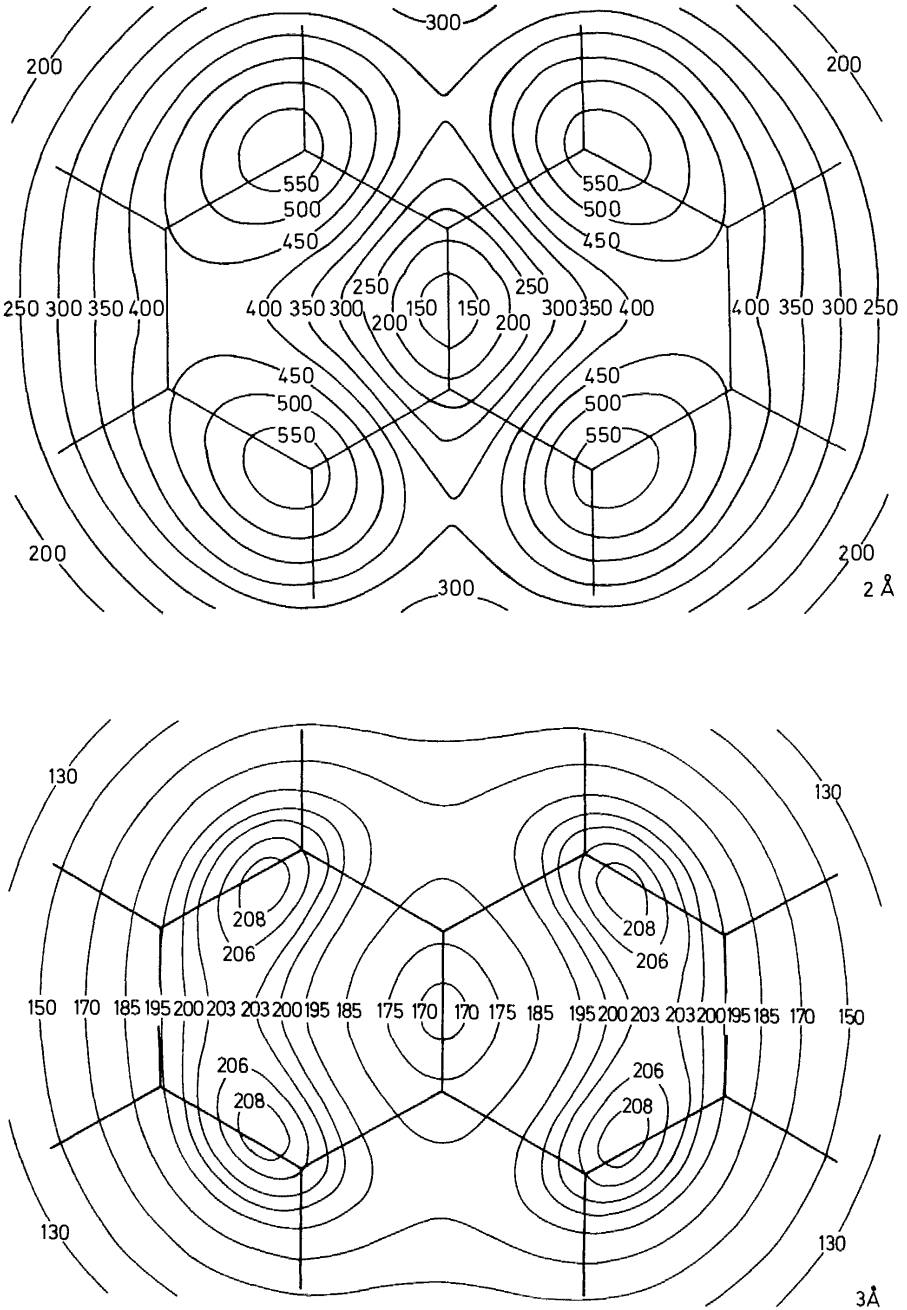

Figure 4. Contour curves of $B_{Ar}/h\gamma_N$ (in gauss) at 2 Å and 3 Å distance from the molecular plane of the NI anion

$\bar{B}$ value with the theoretically calculated B_{Ar} presented in *Figures 4* and 5*. In *Figure 4* contour curves of $B_{Ar}/\hbar\gamma_N$ are given at 2 Å and 3Å distance from the molecular plane of the NI anion. *Figure 5* shows how $B_{Ar}/\hbar\gamma_N$ varies as a function of the distance of the alkali ion to the molecular plane. At distances larger than 3 Å, B_{Ar} becomes almost independent of the position of the alkali ion.

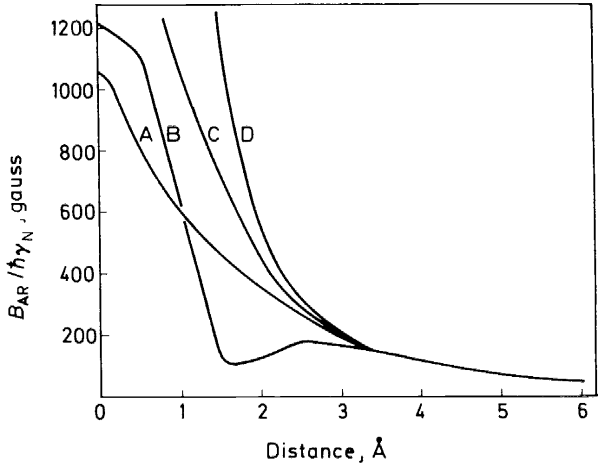

Figure 5. $B_{Ar}/\hbar\gamma_N$ as a function of the distance to the molecular plane of the NI anion. A, above the centre of a benzene ring; B, above the centre of the anion; C, above a C_β atom; D, above a C_α atom

Crystallographic results for single crystals of diamagnetic alkali aromatic compounds by Stucky and co-workers[16] revealed that a distance of 2.0–2.5 Å may be quite reasonable. A recent structure analysis of K_2COT, diglyme (COT = cyclooctatetraene, diglyme = $CH_3(OCH_2CH_2)_2OCH_3$) revealed a distance of 2.45 Å between the cation and the centre of the planar COT dianion[17]. Interestingly, one of the potassium ions is on one side surrounded by a diglyme molecule and on the other side shielded by the planar COT dianion, whereas the other potassium ion is shielded on both sides by COT dianions. The latter potassium ions form a one-dimensional array through the crystal.

The decreasing interionic distance with increasing temperature strongly increases the h.f.s.c. and the $\bar{B}$ value of Li. Therefore, going to higher temperature the line width increases although η_0/T decreases.

NaNI. $T_{2,Fc}^{-1}$ has been calculated from the data in *Table 4*. Since only one isotope could be measured, the magnetic relaxation contributions could

* In refs. 4d and 6b the procedure for calculating the interionic distance has been outlined. It has been shown that B consists of two parts, B_M and B_{Ar}; B_M arises from unpaired spin density at the metal nucleus, B_{Ar} from unpaired spin density in the aromatic part of the ion pair. However, for Li and Na, B_M is small compared with B_{Ar}.

Table 7. Line width analysis results (in rad/s) for NaNl in DME (1.0 M)

Temperature	T_2^{-1}	$T_{2,\mathrm{Fc}}^{-1}$	$T_{2,\mathrm{Dip}}^{-1} + T_{2,\mathrm{Q}}^{-1}$
30°C	1200 ± 100	220 ± 30	1000 ± 100
60°C	2600 ± 200	700 ± 100	1900 ± 300

not be separated from the quadrupolar contribution[6]. The results of the line width analysis are summarized in *Table 7*.

From the ^{23}Na line width of $NaB\phi_4$ in THF[18], of $NaBH_4$ and $NaB\phi_4$ in polyethers[8] and of NaBp in DME[4], one may expect that the contribution of the quadrupolar relaxation to the sodium line width of the NaNl ion pair is of the order of 150–250 rad/s at room temperature. Assuming the same τ_r and the same field gradient at the alkali nucleus for the NaNl as for the KNl ion pair in DME (vide infra), one calculates for $T_{2,\mathrm{Q}}^{-1}$ of ^{23}Na: 170 rad/s at 30°C and 120 rad/s at 60°C. If we now try to calculate from $T_{2,\mathrm{Dip}}^{-1}$ and the upper limit of $\tau_d (= \tau_e)$ the quantity $\bar{B}/\hbar\gamma_N$, we find 820 and 1420 G for NaNl in DME at 30°C and 60°C, respectively. These values are unreasonably high, as can be seen from *Figures 4* and *5*.

Analysing the line width as a function of the concentration, we found that the line width is roughly proportional to $1/c$, which indicates that τ_e is the correlation time which governs the ^{23}Na relaxation. This contrasts with the calculated Fermi contact contribution given in *Table 7*. A way out of this dilemma was found by assuming that the static model for the ion pair is not applicable. Instead of equation (13) the general equations (11) should be applied, which will result in an increase of the Fermi contact relaxation. Assuming a rapid equilibrium between a contact and a solvent-separated ion pair and setting $\tau_e' = \tau_e$ (upper limit), we found for the Fermi contact relaxation 1400 rad/s and 2000 rad/s at 30°C and 60°C, respectively. In this calculation $A_1 = 0$ (solvated ion pair) and A_2 (contact ion pair) was set equal to the limiting value of the ^{23}Na h.f.s.c. observed for NaNl in tetrahydrofuran[19]. Additional evidence for the applicability of the dynamic ion pair description provides the unreasonably low value obtained for k_e calculated from the sodium line width and using equation (13a). For instance, from the data of Figure 5 of ref. 5b (which are essentially in agreement with our experimental results) we calculate $k = 2 \times 10^9$ l/mol.s, whereas ^{1}H n.m.r. (this work) and e.s.r. measurements revealed 14×10^9 l/mol.s.

In conclusion, evidence exists that the Fermi contact relaxation dominates the relaxation of the ^{23}Na nucleus and that the dynamic model holds for describing the configurational changes of the NaNl ion pairs.

KNl. The almost linear relationship between T_2^{-1} and η_0/T (see ref. 6, Figure 8) is characteristic for a contact ion pair whose structure hardly

Table 8. Line width analysis results (in rad/s) for KNl in DME at 30°C (1.0 M)

T_2^{-1}	$T_{2,\mathrm{Fc}}^{-1}$	$T_{2,\mathrm{Dip}}^{-1}$	$T_{2,\mathrm{Q}}^{-1}$
800 ± 60	1.2 ± 0.1	25 ± 5	770 ± 70

changes with the temperature. In *Table 8* the various contributions to the line width have been tabulated. The Fermi contact contribution has been calculated by use of the data of *Table 4*; the dipolar contribution has been calculated with τ_e as an upper limit for τ_d and 1000 G as an upper limit for $\bar{B}/\hbar\gamma_N$. The remaining part of the line width is ascribed to the quadrupolar relaxation.

The q.c.c. calculated from $T_{2,Q}^{-1}$ lies in the range 2.0–4.5 MHz if we use the τ_r values of *Table 4*. This value is comparable to the values reported for some ionic potassium compounds[20]. In order to gain some information about the quadrupolar relaxation of the other alkali nuclei, an estimate was made assuming that τ_r and the electric field gradient at the alkali nucleus remain the same for all alkali NI ion pairs, the Sternheimer shielding factors[4,6] being taken into account (see *Table 9*). The predicted $T_{2,Q}^{-1}$ for the Li nuclei appears to be negligible, in agreement with the results of the ^{6}Li and ^{7}Li line width analysis.

Table 9. Predicted quadrupole line widths (in rad/s) for the alkali resonances of the alkali NI ion pairs in DME

Nucleus	^{6}Li	^{7}Li	^{23}Na	^{39}K	^{85}Rb	^{87}Rb	^{133}Cs
$T_{2,Q}^{-1}$	0.0	0.3	172	770	13300	12900	5

RbNI. Since two isotopes can be studied, a complete line width analysis can be given[6]. The data of *Table 10* demonstrate that the anisotropic magnetic dipolar relaxation is quite unimportant and that the quadrupolar relaxation governs the ^{85}Rb line width for almost 100 per cent and the ^{87}Rb line for about 85 per cent. Comparison of the measured $T_{2,Q}^{-1}$ with the predicted one (see *Table 9*) shows that the field gradient or τ_r is smaller for the RbNI ion pair than for the KNI ion pair. From $T_{2,Q}^{-1}$ one calculates for the q.c.c. of ^{85}Rb and ^{87}Rb 5.7–12.8 MHz and 2.7–6.2 MHz, respectively. Both values fall within the expected range [4, 20]

In accordance with the predominance of the quadrupolar relaxation, the Rb line width is mainly determined by the change in η_0/T (see ref. 6, Figure 7). The predicted Fermi contact relaxation is equal to the experimentally determined contribution of the magnetic relaxation mechanisms. This agreement excludes the applicability of the dynamic model for structural changes of an ion pair as an explanation for the temperature dependence of the Rb h.f.s.c. (see ref. 6, Figure 5).

CsNI. The Cs line width varies linearly with η_0/T (see ref. 6, Figure 7), which points to the existence of a contact ion pair whose structure is not very temperature-dependent. Since the quadrupole moment of Cs is equal to

Table 10. Line width analysis results (in rad/s) for RbNI in DME at 30°C (1.0 M)

Isotope	T_2^{-1}	$T_{2,Q}^{-1}$	$T_{2,Fc}^{-1} + T_{2,Dip}^{-1}$	$T_{2,Fc}^{-1}$
^{85}Rb	7800 ± 200	7700 ± 200	100 ± 40	110 ± 30
^{87}Rb	8700 ± 400	7500 ± 200	1200 ± 400	1000 ± 300

-0.004 barns[21], the quadrupole contribution to the line width can be neglected (see *Table 9*). From the data in *Table 4* one calculates for $T_{2,Fe}^{-1} = 9100 \pm 300$ rad/s, so that the line width is mainly determined by this interaction.

5. CONCLUSION

The available results of n.m.r. studies of ion pairs are promising. The method proves to be applicable for studies of alkali radical salts in concentrated solutions (0.1 – 2.5 M). The spectra provide information on magnitude and sign of the h.f.s.c. Correlation times can be deduced from the spectra. From studying the solutions as a function of concentration spin exchange rates can be inferred, which are in agreement with the rates obtained by e.s.r. In particular the alkali resonance experiments provide information about the structure of the ion pairs.

ACKNOWLEDGEMENTS

The authors wish to thank Dr G. W. Canters for valuable discussions.

This investigation was supported in part by the Netherlands Foundation for Chemical Research (SON), with financial aid from the Netherlands Organization for the Advancement of Pure Research (ZWO).

REFERENCES

[1] For references to earlier work see *Ions and Ion Pairs in Organic Reactions*, Ed. M. Szwarc, Vol. 1, Chapters 5 and 8. Wiley–Interscience; New York (1972).
[2] See Chapter 7 of ref. 1.
[3] (a) R. W. Kreilick, *J. Amer. Chem. Soc.* **90**, 2711 (1968);
(b) G. W. Canters, B. M. P. Hendriks, J. W. M. de Boer and E. de Boer, *Mol. Phys.* **25**, 1135 (1973).
[4] (a) G. W. Canters and E. de Boer, *Mol. Phys.* **13**, 395 (1967);
(b) G. W. Canters, *Thesis*, University of Nijmegen, Nijmegen, The Netherlands (1969);
(c) G. W. Canters and E. de Boer, *Mol. Phys.* **26**, 1185 (1973);
(d) G. W. Canters and E. de Boer, *Mol. Phys.*, **27**, 665 (1974).
[5] (a) T. Takeshita and N. Hirota, *Chem. Phys. Letters*, **4**, 369 (1969);
(b) T. Takeshita and N. Hirota, *J. Chem. Phys.* **58**, 8745 (1973).
[6] (a) B. M. P. Hendriks, G. W. Canters, C. Corvaja, J. W. M. de Boer and E. de Boer, *Mol. Phys.* **20**, 193 (1971);
(b) B. M. P. Hendriks, *Thesis*, University of Nijmegen, Nijmegen, The Netherlands (1973).
[7] G. E. Pake and T. R. Tuttle Jr, *Phys. Rev. Letters*, **3**, 423 (1959).
[8] G. W. Canters, *J. Amer. Chem. Soc.* **94**, 5230 (1972).
[9] V. Vand. *J. Phys. Chem.* **52**, 277 (1948).
[10] E. de Boer and H. van Willigen, *Progress in Nuclear Magnetic Resonance Spectroscopy*, Vol. 2, Chapter 3. Eds. J. W. Emsley, J. Feeney and L. M. Sutcliffe. Pergamon: Oxford (1967).
[11] H. M. McConnell and D. B. Chesnut, *J. Chem. Phys.* **28**, 107 (1958).
[12] (a) A. Abragam, *The Principles of Nuclear Magnetism* Chapter VIII. Oxford University Press: London (1961);
(b) J. A. M. van Broekhoven, B. M. P. Hendriks and E. de Boer, *J. Chem. Phys.* **54**, 1988 (1971).
[13] P. Debye, *Polar Molecules*, Dover, New York (1945).
[14] J. C. Danner, *Thesis*, Brandeis University, Waltham, Mass. (1966).
[15] G. W. Canters, C. Corvaja and E. de Boer, *J. Chem. Phys.* **54**, 3026 (1971).

[16] (a) J. J. Brooks and G. D. Stucky, *J. Amer. Chem. Soc.* **94**, 7333 (1972);
(b) J. J. Brooks, W. Rhine and G. D. Stucky, *J. Amer. Chem. Soc.* **94**, 7339 (1972);
(c) J. J. Brooks, W. Rhine and G. D. Stucky, *J. Amer. Chem. Soc.* 94, 7346 (1972).
[17] J. H. Noordik, Th. E. M. van den Hark, J. J. Mooij and A. A. K. Klaassen, *Acta Cryst.*, **B.30**, 833 (1974).
[18] A. M. Grotens, J. Smid and E. de Boer, *Chem. Commun.* 759 (1971).
[19] N. Hirota, *J. Amer. Chem. Soc.* **90**, 3603 (1968).
[20] (a) M. H. Cohen and F. Reif, 'Quadrupole Effects in NMR Studies of Solids', in *Solid State Effects,* Eds F. Seitz and D. Turnbull, Vol. 5. Academic Press: New York (1957);
(b) T. P. Das and E. L. Hahn, 'Nuclear Quadrupole Spectroscopy', in *Solid State Effects,* Eds F. Seitz and D. Turnbull, Vol. 5. Academic Press: New York (1957), supplement 1, (1958).
[21] (a) P. Buck, I. I. Rabi and B. Senitzky, *Phys. Rev.* **104**, 513 (1956);
(b) H. Bucka, H. Kopferman and E. W. Otten, *Ann. Phys.* 4, 39 (1959).